LETTERS

Phosphorylation of histone H3T6 by PKCβI controls demethylation at histone H3K4

Eric Metzger[1], Axel Imhof[3], Dharmeshkumar Patel[1], Philip Kahl[4], Katrin Hoffmeyer[1], Nicolaus Friedrichs[1], Judith M. Müller[1], Holger Greschik[1], Jutta Kirfel[4], Sujuan Ji[1], Natalia Kunowska[1], Christian Beisenherz-Huss[2], Thomas Günther[1], Reinhard Buettner[4] & Roland Schüle[1]

Demethylation at distinct lysine residues in histone H3 by lysine-specific demethylase 1 (LSD1) causes either gene repression or activation[1,2]. As a component of co-repressor complexes, LSD1 contributes to target gene repression by removing mono- and dimethyl marks from lysine 4 of histone H3 (H3K4)[1,3]. In contrast, during androgen receptor (AR)-activated gene expression, LSD1 removes mono- and dimethyl marks from lysine 9 of histone H3 (H3K9)[2]. Yet, the mechanisms that control this dual specificity of demethylation are unknown. Here we show that phosphorylation of histone H3 at threonine 6 (H3T6) by protein kinase C beta I (PKCβI, also known as PRKCβ) is the key event that prevents LSD1 from demethylating H3K4 during AR-dependent gene activation. In vitro, histone H3 peptides methylated at lysine 4 and phosphorylated at threonine 6 are no longer LSD1 substrates. In vivo, PKCβI co-localizes with AR and LSD1 on target gene promoters and phosphorylates H3T6 after androgen-induced gene expression. RNA interference (RNAi)-mediated knockdown of PKCβI abrogates H3T6 phosphorylation, enhances demethylation at H3K4, and inhibits AR-dependent transcription. Activation of PKCβI requires androgen-dependent recruitment of the gate-keeper kinase protein kinase C (PKC)-related kinase 1 (PRK1)[4]. Notably, increased levels of PKCβI and phosphorylated H3T6 (H3T6ph) positively correlate with high Gleason scores of prostate carcinomas, and inhibition of PKCβI blocks AR-induced tumour cell proliferation in vitro and cancer progression of tumour xenografts in vivo. Together, our data establish that androgen-dependent kinase signalling leads to the writing of the new chromatin mark H3T6ph, which in consequence prevents removal of active methyl marks from H3K4 during AR-stimulated gene expression.

We previously showed that during AR-dependent gene activation, LSD1 co-operates with a trimethyl demethylase, the Jumonji C (JMJC)[5] domain-containing protein JMJD2C (also known as KDM4C), in removing repressive histone marks from H3K9 (ref. 6). This process is controlled by the upstream gatekeeper kinase, PRK1 (also known as PKN1)[4]. However, it has remained elusive how the demethylase activity of LSD1 is obstructed from demethylating H3K4 at AR-regulated genes. Our analysis of the reported crystal structures of LSD1 in complex with histone H3 peptides[7,8] suggested that phosphorylation of H3T6 in the proximity of H3K4 might interfere with LSD1-mediated H3K4 demethylation (Supplementary Fig. 1).

To screen for H3T6 kinases, we incubated nucleosomes purified from HeLa cells with 97 kinases (Supplementary Figs 2 and 3). Western blot analysis performed with an anti-H3T6ph antibody demonstrates that only PKCα, βI and βII phosphorylate nucleosomes

at H3T6 (Fig. 1a and Supplementary Figs 3 and 4a). PKCα, βI and βII specifically target H3T6 but not H3T3, H3S10 or H3T11 (Fig. 1a). Because LNCaP human prostate cancer cells express PKCβI only, we continued all further studies with PKCβI (Supplementary Fig. 4b). To corroborate that PKCβI exclusively phosphorylates H3T6, we
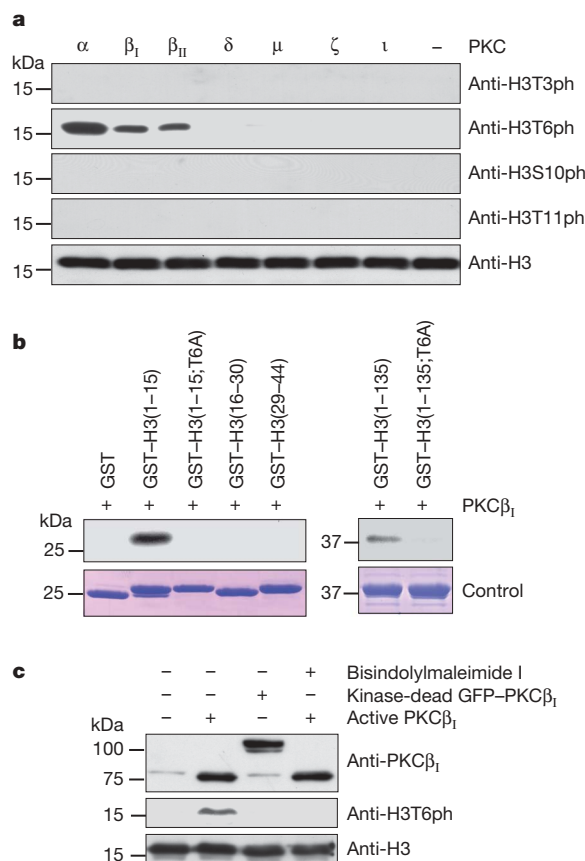
Figure 1 | PKCα, βI and βII specifically phosphorylate H3T6.
a, b, Nucleosomes from HeLa cells (a) or bacterially expressed GST and GST–H3 proteins (b) were incubated with active PKCα, βI, βII, δ, μ, ζ or ι as indicated. Coomassie blue staining (b, bottom) shows the amounts of GST-fusion proteins used. c, In 293T cells, H3T6 is phosphorylated by active PKCβI but not by a kinase-dead mutant or in the presence of the inhibitor bisindolylmaleimide I. Western blots were probed with the indicated antibodies (a, c).

[1]Urologische Klinik/Frauenklinik und Zentrale Klinische Forschung, Klinikum der Universität Freiburg, Breisacherstrasse 66, [2]ProQinase, Breisacherstrasse 117, 79106 Freiburg, Germany. [3]Adolf-Butenandt Institute and Munich Center of Integrated Protein Science (CIPS), Ludwig Maximilians University of Munich, Schillerstrasse 44, 80336 Munich, Germany. [4]Institut für Pathologie, Universitätsklinikum Bonn, Sigmund-Freud-Strasse 25, 53127 Bonn, Germany.

incubated PKCβ$_I$ with glutathione S-transferase (GST)–H3 or GST control proteins in the presence of [γ-^{32}P]ATP. Only full-length histone H3 (H3(1–135)) and an H3 fragment spanning amino acid residues 1 to 15 (H3(1–15)) are phosphorylated by PKCβ$_I$ (Fig. 1b). Furthermore, mutation of threonine 6 to alanine in either the H3 fragment (H3(1–15;T6A)) or the full-length H3 (H3(1–135;T6A)) abolishes phosphorylation, demonstrating that PKCβ$_I$ targets H3T6 only (Fig. 1b).

Next, we tested the ability of PKCβ$_I$ to phosphorylate H3T6 in vivo. 293T cells were transfected with plasmid expressing either a constitutively active or a kinase-dead PKCβ$_I$ mutant in the presence or absence of the PKCβ$_I$ inhibitor bisindolylmaleimide I and subjected to western blot analysis (Fig. 1c). H3T6 is phosphorylated only in cells expressing active PKCβ$_I$, but not in cells expressing kinase-dead PKCβ$_I$ or in cells treated with inhibitor. Taken together, our data identify PKCβ$_I$ as the first H3T6 kinase.

To test our hypothesis that phosphorylation of H3T6 interferes with demethylation at H3K4, we performed in vitro demethylation assays. Di- and monomethyl H3K4 peptides either unmodified at Thr 6 (H3K4me2 and H3K4me1) or phosphorylated at Thr 6 (H3K4me2T6ph and H3K4me1T6ph) were incubated with LSD1 and analysed by mass spectrometry (Fig. 2a, b and Supplementary Fig. 4c). The robust demethylation of H3K4me2 observed in the presence of LSD1 results in the loss of one or two methyl groups (me), converting K4me2 into mono- or unmethylated lysine (Fig. 2a). Importantly, demethylation is completely blocked when the peptides are phosphorylated at Thr 6 (Fig. 2a). Likewise, demethylation of H3K4me1 by LSD1 is completely abrogated in the presence of phosphorylated Thr 6 (Fig. 2b). Next, we asked whether phosphorylation of core histones or nucleosomes at H3T6 blocks demethylation of H3K4me2 by LSD1. Core histones and nucleosomes were first phosphorylated by PKCβ$_I$ and then subjected to demethylation by LSD1. Phosphorylation of core histones or nucleosomes at H3T6 blocks demethylation of H3K4me2 by LSD1 but does not affect demethylation of H3K9me2 (Fig. 2c, d and Supplementary Fig. 4d).

Because LSD1 only removes mono- and dimethyl marks[1,2], we wondered whether phosphorylation of H3T6 also blocks demethylation of H3K4me3 and H3K4me2 by JMJC domain-containing demethylases such as JARID1B (also known as KDM5B)[9]. JARID1B efficiently demethylates H3K4me3 and H3K4me2 peptides (Supplementary Figs 4e and 5). Indeed, demethylation of tri- and dimethyl H3K4 peptides phosphorylated at Thr 6 (H3K4me3T6ph and H3K4me2T6ph) is severely impaired (Supplementary Fig. 5). These results demonstrate that phosphorylation of H3T6 blocks demethylation of H3K4 methyl marks by LSD1 and JARID1B in vitro.
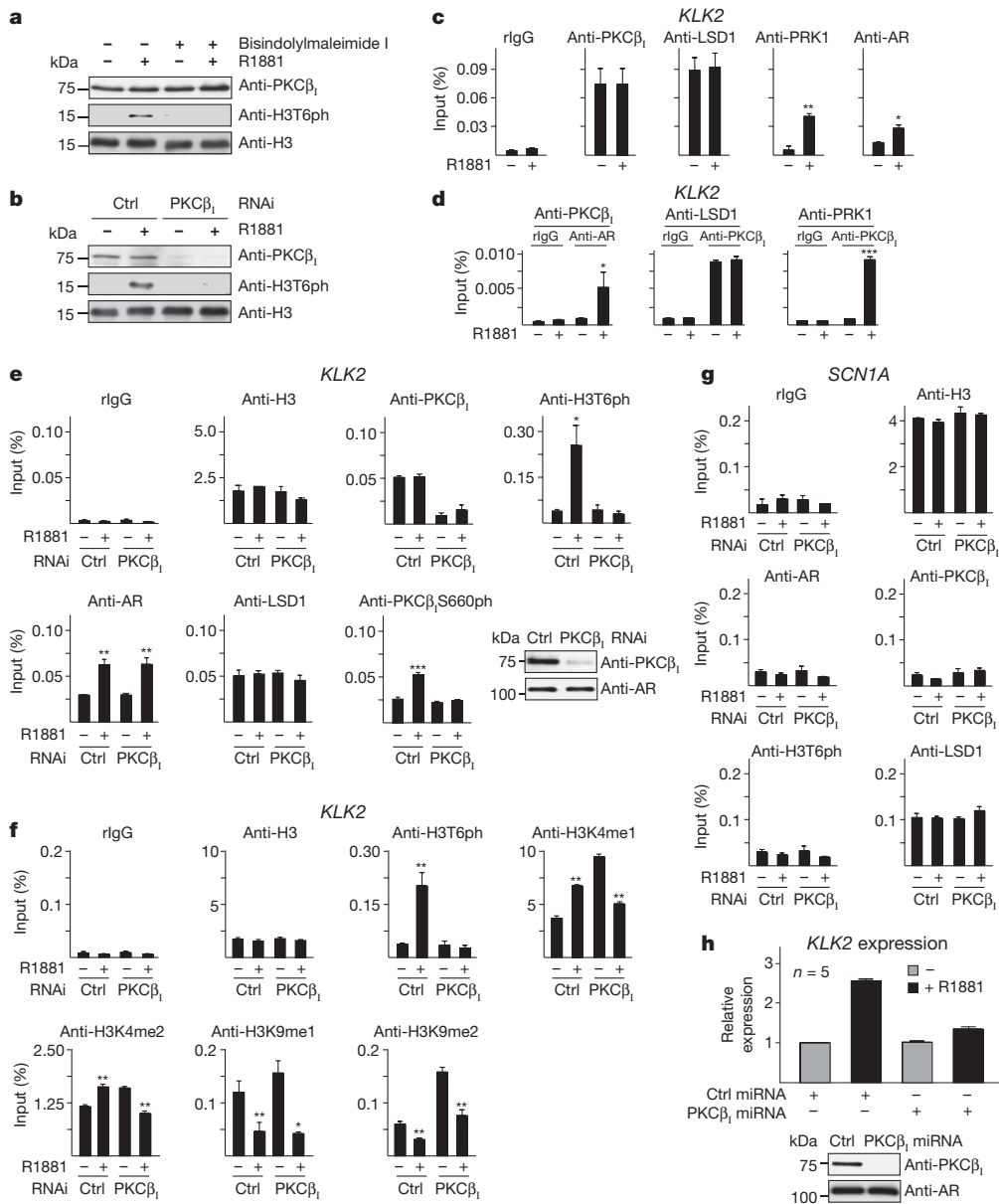
During AR-dependent gene expression, demethylation of active H3K4 methyl marks by LSD1 must be prevented. To test whether H3T6 is phosphorylated during AR signalling we treated LNCaP cells with the AR agonist R1881. Notably, nucleosomes isolated from LNCaP cells treated with R1881 are phosphorylated at H3T6, demonstrating that phosphorylation of H3T6 occurs in a ligand-dependent manner in vivo (Fig. 3a). The ligand-induced phosphorylation is specifically blocked either by treating the cells with PKCβ$_I$ inhibitor or by knockdown of PKCβ$_I$ (Fig. 3a, b). Next, we analysed whether PKCβ$_I$ is present at AR target genes. LNCaP cells were subjected to chromatin immunoprecipitation (ChIP) in the presence or absence of R1881. PKCβ$_I$ specifically associates with the androgen response elements (AREs) located in the promoters or enhancers of the KLK2 (ref. 10), FKBP5 (ref. 11), TMPRSS2 (ref. 12) and ELK4 (ref. 13) genes (Fig. 3c and Supplementary Figs 6 and 7a). PKCβ$_I$ binds to chromatin in a ligand-independent manner similar to LSD1 (ref. 2; Fig. 3c and Supplementary Figs 6 and 7a). In comparison, PRK1 and AR bind chromatin only in a ligand-dependent manner (Fig. 3c and Supplementary Figs 6 and 7a). AR, LSD1 and PKCβ$_I$ are also present on AR target gene promoters in AR-positive LAPC4 but not in AR-negative PC3 prostate tumour cells, or in other tested cell lines
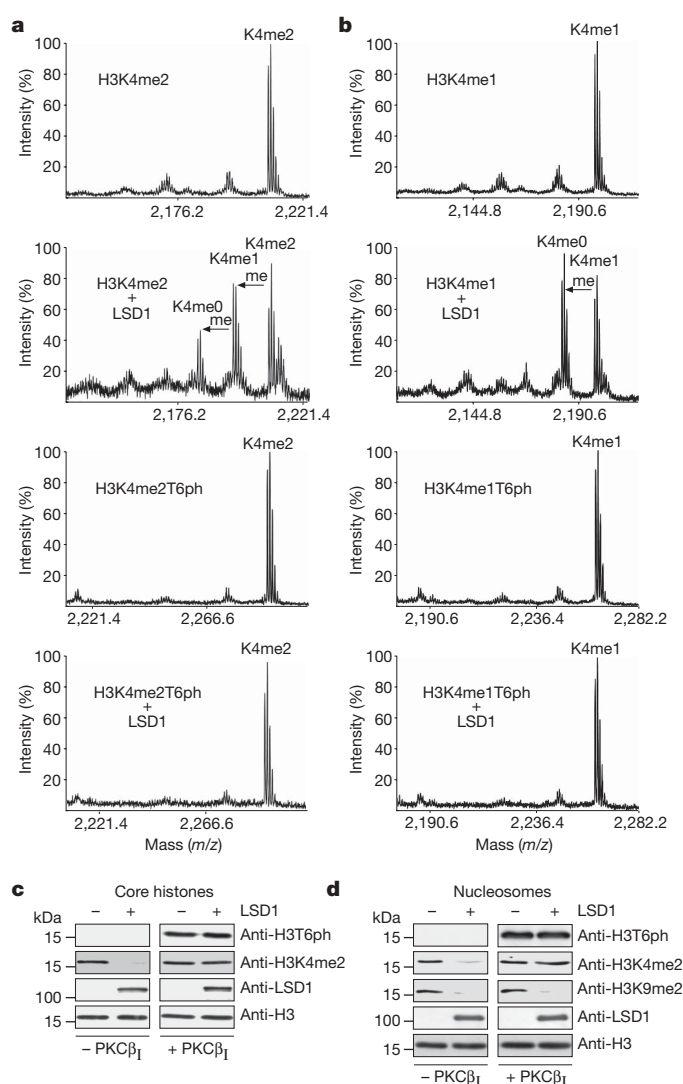
Figure 2 | Phosphorylation of H3T6 blocks demethylation at H3K4 by LSD1. a, b, H3K4me2 or H3K4me2T6ph (**a**) and H3K4me1 or H3K4me1T6ph (**b**) peptides corresponding to the H3 tail residues 1–20 were incubated in the presence or absence of LSD1, and analysed by mass spectrometry. A shift in mass equivalent to one methyl group is indicated as 'me'. **c, d,** For demethylation assays, untreated core histones (**c**, left) or nucleosomes (**d**, left) and core histones or nucleosomes phosphorylated by recombinant PKCβ$_I$ at H3T6 in vitro (**c, d**, right) were incubated with bacterially expressed and purified His–LSD1. Western blots were probed with the indicated antibodies.

(Supplementary Figs 8–11). Because PKCβ$_I$ interacts with LSD1 and AR (Supplementary Fig. 12a, b, d) we investigated by sequential chromatin immunoprecipitation (re-ChIP) whether PKCβ$_I$, LSD1 and AR are present in the same complex on the KLK2 and FKBP5 promoters. In LNCaP cells, PKCβ1 and AR form a complex on chromatin after addition of R1881 (Fig. 3d, left and Supplementary Fig. 7b), whereas PKCβ$_I$ and LSD1 associate on chromatin in a ligand-independent manner (Fig. 3d, middle and Supplementary Fig. 7b).

Next, we asked whether PKCβ$_I$ phosphorylates H3T6 at promoters of AR-regulated genes in vivo. LNCaP cells, cultured in the presence or absence of R1881, were transfected with either an unrelated control short interfering RNA (siRNA) or an siRNA directed against PKCB1, and then subjected to ChIP with an anti-H3T6ph antibody. Notably, addition of ligand results in phosphorylation of H3T6 at the AREs of the KLK2, FKBP5, TMPRSS2 and ELK4 promoters or enhancers (Fig. 3e and Supplementary Figs 7c and 13). Androgen-induced phosphorylation of H3T6 is PKCβ$_I$-dependent as it is specifically blocked by PKCβ$_I$ knockdown (Fig. 3e and Supplementary Figs 7c

Figure 3 | PKCβ_I phosphorylates H3T6 and controls demethylation at H3K4 during AR-dependent gene expression. a, b, In LNCaP cells, R1881 specifically induces phosphorylation of H3T6, which is blocked by bisindolylmaleimide I (**a**) or by RNAi-mediated knockdown of PCKβ_I (**b**). Ctrl, control. **c–g,** For ChIP (**c, e–g**) and re-ChIP (**d**), LNCaP cells were cultivated in the presence or absence of the AR agonist R1881, and transfected with siRNA (**e–g**), as indicated. ChIP analyses were performed with the indicated antibodies. The precipitated chromatin was quantified by quantitative PCR (qPCR) analysis using primers flanking AREs in the promoter of the *KLK2* gene or primers in the promoter of the *SCN1A* gene, as indicated. Data are mean + s.e.m. ($n \geq 3$). *$P < 0.005$, **$P < 0.001$, ***$P < 0.0001$, in comparison to cells treated without (−) R1881. **h,** microRNA (miRNA)-mediated PKCβ_I knockdown reduces expression of the androgen-regulated *KLK2* gene in LNCaP cells. Western blots (**a, b, e, h**) were probed with the indicated antibodies.

and 13). PKCβ_I depletion does not affect the ligand-dependent recruitment of AR, or the presence of LSD1 on AR-regulated genes (Fig. 3e and Supplementary Figs 7c and 13). Because PKCβ_I is present on the AREs of AR target genes irrespective of the presence or absence of ligand, whereas H3T6 phosphorylation is only observed in the presence of R1881, we asked whether PKCβ_I is activated in an androgen-dependent manner. Active PKCβ_I is characterized by autophosphorylation of Ser 660 (S660ph)[14]. ChIP assays using an anti-PKCβ_I S660ph antibody show androgen-induced phosphorylation of PKCβ_I at the AREs of the *KLK2*, *FKBP5*, *TMPRSS2* and *ELK4* genes (Fig. 3e and Supplementary Figs 7c and 13). Taken together, these data demonstrate androgen-dependent activation of PKCβ_I and phosphorylation of H3T6 by PKCβ_I *in vivo*.

We recently showed that PRK1 is a gatekeeper for regulation of AR target gene expression that phosphorylates H3T11 (ref. 4). Because PKCβ_I and PRK1 interact (Supplementary Fig. 12c, d), we tested whether both kinases are present in the same complex at promoters of AR target genes. Re-ChIP analysis demonstrates that after ligand addition both proteins form a complex on the *KLK2* and *FKBP5* promoters (Fig. 3d, right and Supplementary Fig. 7b). Next, we investigated whether PRK1 regulates PKCβ_I activity. LNCaP cells, grown in the presence or absence of R1881, were depleted of PRK1 and then subjected to ChIP. Ligand-dependent activation of PKCβ_I is blocked by knockdown of PRK1 (Supplementary Fig. 7d, e). Consequently, ligand-dependent phosphorylation of H3T6 at the AREs of the *KLK2* and *FKBP5* promoters is abolished

(Supplementary Fig. 7d, e). On the other hand, PKCβ$_I$ knockdown does not influence ligand-dependent recruitment of PRK1 or PRK1-mediated phosphorylation of H3T11 at AR target promoters (Supplementary Fig. 14). Thus, our data suggest that PRK1 functions upstream of PKCβ$_I$, although we do not observe direct phosphorylation of PKCβ$_I$ by PRK1 (Supplementary Fig. 12e). In summary, these data demonstrate that PKCβ$_I$ phosphorylates H3T6 at AR target gene promoters in an androgen- and PRK1-dependent manner.

Because ligand-dependent expression of AR target genes requires removal of repressive methyl marks from H3K9 (ref. 2), but demands the maintenance of active methyl marks at H3K4 (ref. 15), we analysed whether phosphorylation of H3T6 by PKCβ$_I$ prevents demethylation of H3K4me1/2 by LSD1 during androgen induced transcription *in vivo*. LNCaP cells were cultivated with or without R1881, depleted of PKCβ$_I$, and subjected to ChIP. Levels of H3K4me1/2 observed at the *KLK2* and *FKBP5* promoters in the absence of ligand are increased after the addition of R1881 (Fig. 3f and Supplementary Fig. 7f), which is in agreement with previous data[15]. Furthermore, the ligand-dependent increase in H3K4me1/2 correlates with R1881-induced phosphorylation of H3T6 by PKCβ$_I$. Knockdown of PKCβ$_I$ blunts ligand-induced phosphorylation of H3T6 and, importantly, allows demethylation of H3K4me1/2 in the presence of R1881 (Fig. 3f and Supplementary Fig. 7f). Treatment of the cells with the PRK1 inhibitor Ro318220 also blunts ligand-induced phosphorylation of H3T6 and reduces H3K4me2 levels (Supplementary Fig. 15). In contrast, ligand-induced demethylation of H3K9me1/2 (ref. 2) is not blocked by PKCβ$_I$ knockdown (Fig. 3f and Supplementary Fig. 7f). Comparable data are obtained with the *TMPRSS2* and *ELK4* enhancers (Supplementary Fig. 13). Together, our observations show that phosphorylation of H3T6 by PKCβ$_I$ interferes with the removal of H3K4 methyl marks by LSD1 *in vivo*. Notably, increased levels of H3K4me1/2 are observed after PKCβ$_I$ knockdown in the absence of R1881, indicating androgen-independent functions of PKCβ$_I$ beyond phosphorylation of H3T6 (Fig. 3f and Supplementary Fig. 7f). Next, we tested whether PKCβ$_I$ signalling also occurs on genes such as *SCN1A* or *SCN2A* in which LSD1 removes active H3K4 methyl marks to silence gene expression[1]. ChIP assays show that opposite to AR-activated genes, PKCβ$_I$ does not associate with LSD1-silenced genes and consequently H3T6 is not phosphorylated (Fig. 3g and Supplementary Figs 7g and 11d).

We then analysed the effect of PKCβ$_I$ knockdown on the expression of AR target genes in LNCaP cells. Quantitative RT–PCR analyses show that the reduction of PKCβ$_I$ levels strongly and specifically impairs androgen-induced expression of endogenous AR target genes (Fig. 3h and Supplementary Fig. 16). In addition, treatment of LNCaP cells with PKCβ$_I$ inhibitor blocks ligand-induced expression of AR target genes only (Supplementary Fig. 17). Altogether, our data demonstrate that PKCβ$_I$ signalling to chromatin prevents LSD1 from demethylating active H3K4 marks during AR-regulated gene expression, thus introducing H3T6ph as a new chromatin mark for transcriptional activation.

Next, we analysed the levels of PKCβ$_I$, H3T6ph and H3K4me2 by immunostaining a panel of 25 normal human prostates and 154 prostate carcinomas on tissue microarrays (Fig. 4a–d). PKCβ$_I$ and H3T6ph are present in the nuclei of epithelial cells of human normal prostate and prostate tumour cells (Supplementary Fig. 18a–c). Quantification of immunoreactivity of the normal human prostates and prostate carcinomas by scoring staining intensity and the percentage of positive carcinoma cells[16] shows that high PKCβ$_I$, H3T6ph and H3K4me2 levels significantly correlate with high Gleason scores and indicate aggressive biology of the tumours (Fig. 4b–d and Supplementary Figs 18d and 19). To examine whether PKCβ$_I$ regulates tumour cell proliferation, we quantified androgen-dependent proliferation of LNCaP cells after PKCβ$_I$ depletion. Androgen-induced proliferation of LNCaP cells is severely reduced by PKCβ$_I$ knockdown when compared to control cells (Fig. 4e and Supplementary Fig. 20). Finally, we analysed the effect of PKCβ$_I$
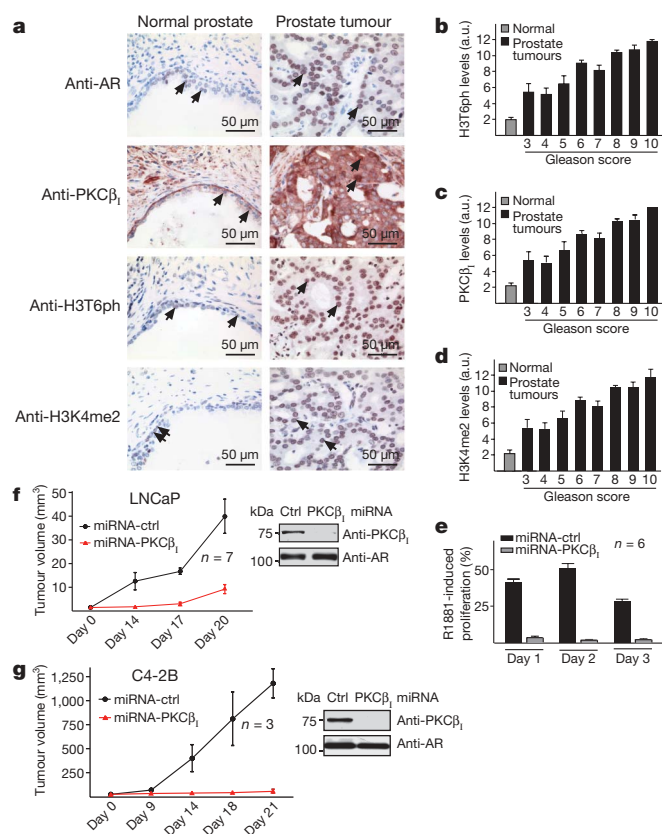
Figure 4 | **PKCβ$_I$, H3T6ph and H3K4me2 levels positively correlate with the malignancy of prostate cancer, and PKCβ$_I$ controls androgen-dependent tumour cell proliferation and cancer growth in tumour xenografts. a**, Immunohistochemical staining of AR, PKCβ$_I$, H3T6ph and H3K4me2 in human normal and tumour (Gleason score 9) prostate. AR, PKCβ$_I$, H3T6ph and H3K4me2 immunoreactivity is detected in the secretory epithelium of normal prostate (arrows, left panels) and prostate carcinoma cells (arrows, right panels). All sections were taken from the same radical prostatectomy specimen. Original magnification, ×250. **b–d**, The correlation of increased H3T6ph (**b**), PKCβ$_I$ (**c**) and H3K4me2 (**d**) levels with high Gleason scores in a panel of 154 human prostate carcinomas is highly significant ($P < 0.0001$). Normal prostate specimens are included as a control. **e**, miRNA-mediated PKCβ$_I$ knockdown severely reduces R1881-induced cell proliferation in LNCaP cells. Data are mean + s.e.m. **f, g**, In mice, the growth of LNCaP (**f**) and C4-2B (**g**) xenograft tumours is severely impaired by PKCβ$_I$ knockdown. Western blots were probed with the indicated antibodies. *n* indicates the number of analysed animals per group. Error bars represent ± s.e.m.

knockdown on tumour cell proliferation *in vivo*. Xenograft mice were generated by implanting LNCaP or C4-2B prostate tumour cells that were specifically depleted of PKCβ$_I$ (Fig. 4f, g and Supplementary Fig. 21). Xenograft tumour growth is significantly reduced after PKCβ$_I$ knockdown, emphasizing the important role of PKCβ$_I$ in the control of prostate tumour cell growth. In conclusion, our data establish that H3T6ph is a new chromatin mark for transcriptional activation. Phosphorylation of H3T6 is executed by PKCβ$_I$ in an androgen-dependent manner, is controlled by the upstream gatekeeper kinase PRK1, and prevents demethylation at H3K4 by LSD1 (Supplementary Fig. 22). Thus, PKCβ$_I$ is a new writer of chromatin marks in the androgen-dependent signalling network and represents a new promising therapeutic target in the treatment of prostate cancer.

METHODS SUMMARY

Cell culture conditions, plasmid construction, methods for cell transfection, chromatin immunoprecipitation, cell proliferation assay, demethylase assay, kinase assay, mass spectrometry analysis, quantitative RT–PCR, western blot, tissue microarrays analysis, and growth of xenograft tumours in mice are described in detail in Methods.

1. Shi, Y. *et al.* Histone demethylation mediated by the nuclear amine oxidase homolog LSD1. *Cell* **119**, 941–953 (2004).
2. Metzger, E. *et al.* LSD1 demethylates repressive histone marks to promote androgen-receptor-dependent transcription. *Nature* **437**, 436–439 (2005).
3. Wang, Y. *et al.* LSD1 is a subunit of the NuRD complex and targets the metastasis programs in breast cancer. *Cell* **138**, 660–672 (2009).
4. Metzger, E. *et al.* Phosphorylation of histone H3 at threonine 11 establishes a novel chromatin mark for transcriptional regulation. *Nature Cell Biol.* **10**, 53–60 (2008).
5. Klose, R. J., Kallin, E. M. & Zhang, Y. JmjC-domain-containing proteins and histone demethylation. *Nature Rev. Genet.* **7**, 715–727 (2006).
6. Wissmann, M. *et al.* Cooperative demethylation by JMJD2C and LSD1 promotes androgen receptor-dependent gene expression. *Nature Cell Biol.* **9**, 347–353 (2007).
7. Yang, M. *et al.* Structural basis of histone demethylation by LSD1 revealed by suicide inactivation. *Nature Struct. Mol. Biol.* **14**, 535–539 (2007).
8. Forneris, F., Binda. C., Adamo, A., Battaglioli, E. & Mattevi, A. Structural basis of LSD1-CoREST selectivity in histone H3 recognition. *J. Biol. Chem.* **282**, 20070–20074 (2007).
9. Metzger, E. & Schüle, R. The expanding world of histone lysine demethylases. *Nature Struct. Mol. Biol.* **14**, 252–254 (2007).
10. Kang, Z., Pirskanen, A., Janne, O. A. & Palvimo, J. J. Involvement of proteasome in the dynamic assembly of the androgen receptor transcription complex. *J. Biol. Chem.* **277**, 48366–48371 (2002).
11. Magee, J. A. *et al.* Direct, androgen receptor mediated regulation of the FKBP5 gene via a distal enhancer element. *Endocrinology* **147**, 590–598 (2005).
12. Wang, Q. *et al.* A hierarchical network of transcription factors governs androgen receptor-dependent prostate cancer growth. *Mol. Cell* **27**, 380–392 (2007).
13. Makkonen, H. *et al.* Identification of ETS-like transcription factor 4 as a novel androgen receptor target in prostate cancer cells. *Oncogene* **27**, 4865–4876 (2008).
14. Keranen, L. M., Dutil, E. M. & Newton, A. C. Protein kinase C is regulated *in vivo* by three functionally distinct phosphorylations. *Curr. Biol.* **5**, 1394–1403 (1995).
15. Kang, Z., Jänne, O. A. & Palvimo, J. J. Coregulator recruitment and histone modifications in transcriptional regulation by the androgen receptor. *Mol. Endocrinol.* **18**, 2633–2648 (2004).
16. Kononen, J. *et al.* Tissue microarrays for high-throughput molecular profiling of tumour specimens. *Nature Med.* **4**, 844–847 (1998).

METHODS

Plasmids. The following plasmids were described previously: pGEX-4T1-H3(1–15), pGEX-4T1-H3(16–30), pGEX-4T1-H3(29–44), pET-GEX-H3(1–135), and pLenti6-miRNA-control[4]. GST–H3(1–135;T6A) was provided by J. M. G. Higgins. To construct GST–H3(1–15;T6A), the corresponding complementary DNA fragment was cloned into pGEX-4T1. To construct pLenti6-miRNA-PKCβI, the DNA corresponding to miRNA-PKCβI (5′-TGCTGTTACGTAGGGATCTGACAGGCGTTTTGGCCACTGACTGACGCCTGTCATCCCTACGTAA-3′ and 5′-CCTGTTACGTAGGGATGACAGGCGTCAGTCAGTGGCCAAAACGCCTGTCAGATCCCTACGTAAC-3′) was cloned into pLenti6/V5-DEST according to the manufacturer's instructions (Invitrogen). Cloning details can be obtained on request.

Chromatin immunoprecipitation. ChIP and re-ChIP experiments were performed as described[4]. LNCaP cells were cultured for 15 min (ChIP) or 210 min (re-ChIP) in the presence or absence of 1×10^{-8} M R1881 or 1×10^{-5} M Ro318220 (Alexis Biochemicals) as indicated. Three days before collection, cells were transfected with siRNA (control for *PKCB1*: 5′-CATTCCTATGCGAGACGTATGTAAA-3′; *PKCB1*: 5′-CATTGTCCTCGTAAGAGATGCTAAA-3′ (Fig. 3e, f, g and Supplementary Fig. 7c, f, g); control for *PRK1*: 5′-GAAAGTCCTAGATCCACACGCAAAT-3′; *PRK1*: 5′-GAACAUGAUCCAGACCUACAGCAAU-3′ (Supplementary Fig. 7d, e); Invitrogen) using RNAifect (Qiagen) following the manufacturer's instructions. Immuno-precipitation was performed with specific antibodies: anti-AR (06-680 lot 33529), anti-H3K9me1 (07-450 lot 24441), anti-H3K9me2 (07-441 lot 30309) (Upstate Biotechnology), anti-H3K4me1 (ab8895 lot 535654), anti-H3T6ph (ab14102 lot 481643), anti-H3 (ab1791 lot 172452), anti-PKCβI S660ph (ab23513 lot 596904) (Abcam), anti-PKCβI (sc-209 lot 481643) (Santa Cruz), anti-H3K4me2 (cs-035-100 lot A391001) (Diagenode), anti-PRK1 (ref. 4), and anti-LSD1 (ref. 2) on protein A-Sepharose 4B (GE-Healthcare). For qPCR, 2 μl out of 50 μl DNA extract was used. qPCR primers for *FKBP5* (+351/+443), *PSA* (−4,288/−3,922), *KLK2* (−343/−90), *SCN1A*, *SCN2A*, *GAPDH* and *U6* (also known as *RNU6-1*) were described previously[1,2,6,11]. qPCR analysis were performed using the LightCycler system (Roche) and ABsolute SYBR green ROX Mix (Thermo Scientific). The data are expressed as mean + s.e.m. Statistical analysis was performed using a two-tailed Student's test. Values of $P < 0.05$ were considered to be statistically significant.

Western blot analysis. Experiments were performed as described[2]. Western blots were probed as indicated.

Cell culture and transfection. LNCaP cells were cultured and transfected as described[2]. PC3 cells were cultured in Ham's F-12 supplemented with 10% FCS and glutamine; HeLa, LAPC4 and MCF7 cells were cultured in DMEM supplemented with 10% FCS and glutamine. LAPC4 cells were cultured in presence of 10^{-7} M dihydrotestosterone (Sigma). Ten micrograms of expression plasmid coding for kinase-dead GFP–PKCβI or constitutively active PKCβI were transfected per dish (Fig. 1c). Three days before collection, cells were transfected with RNAi (Fig. 3b). Cells were cultivated for 48 h in medium supplemented with 0.5% double-stripped FCS, (Figs 1c and 3a, b), treated for 1 h with 1×10^{-4} M bisindolylmaleimide I (Calbiochem) (Fig. 3a) in the presence (15 min) or absence of 1×10^{-8} M R1881 (Sigma) (Fig. 3b), as indicated. Controls (Supplementary Figs 4b, 8a, 9a, 10a, 11a and 18d) show extracts of 293T cell transfected with expression plasmid coding for PKCα, PKCβI or PKCβII.

Cell proliferation assay. Experiments were performed as described[2]. pLenti6-miRNA-control and pLenti6-miRNA-PKCβI were used to produce recombinant lentiviruses to infect LNCaP cells as described[17]. The infected cells were cultured for 72 h in medium containing 10% double-stripped FCS. Ten-thousand cells were plated in a 96-well plate in the presence or absence of 1×10^{-9} M R1881. The cell proliferation ELISA BrdU Colourimetric Assay (Roche) was performed according to the manufacturer's instructions. The figure shows the increase of proliferation in the presence versus absence of R1881. The experiments were performed in hexaplicate.

Quantitative RT–PCR and statistical analysis. Quantitative PCR with reverse transcription (qRT–PCR) and statistical analysis were performed as described[2]. The primers for *GAPDH*, *KLK2* and *FKBP5* were described previously[2,6,11].

***In vitro* kinase assay.** The kinase assays were performed as described[4]. Either 10 μg of GST–H3 proteins (Fig. 1b) or 1 μg of nucleosomes (Fig. 1a) purified from HeLa cells[18] were incubated for 7 min with the amount corresponding to 12 pmol min^{-1} of purified recombinant PKC (ProQinase) at 30 °C in kinase buffer containing 60 mM HEPES-NaOH, pH 7.5, 3 mM MgCl$_2$, 3 mM MnCl$_2$ and either 10 mM ATP (Fig. 1a) or 5 μCi [γ-^{32}P]ATP (Fig. 1b). The reaction mixture was analysed by western blotting using antibodies as indicated (Fig. 1a) or SDS–PAGE followed by autoradiography (Fig. 1b).

Immunohistochemistry. Immunostaining was performed using a protocol[19] for antigen retrieval and indirect immunoperoxidase. Anti-AR (sc-7305 lot E171;

Santa Cruz; 1:75), anti-PKCβI (sc-209 lot 481643; Santa Cruz; 1:1,000), anti-H3T6ph (ab14102 lot 481643; Abcam; 1:200), and anti-H3K4me2 (ab7766-100, lot 56290; Abcam; 1:1,000) antibodies were used. Immunoreactions were performed with the Universal Vectastain ABC kit according to the manufacturer's instructions (Vector Laboratories).

Tissue microarrays and statistical analysis. Clinical data of patients and procedures for generating the tissue microarrays were described previously[19]. Tissue microarrays were prepared from formalin-fixed, paraffin-embedded tissue specimens of 154 prostates selected from the archival files of the Institute of Pathology, University of Bonn Medical School. All tumour samples were surgically obtained from patients who had undergone radical retropubic prostatectomy in two surgical centres between 1995 and 2002 for clinically organ confined prostate cancer (preoperative staging less than or equal to cT2, cNo and cMo according to the UICC classification of tumours). On the basis of preoperative staging there is no evidence for tumour growth beyond the prostate capsule (cT1 or cT2) and no metastatic spread into locoregional lymph nodes (cNo) or distant metastases (cMo). Patients who had received previous hormonal therapy, chemotherapy, or radiation therapy were excluded from our study. All cases were re-evaluated by a panel of experienced pathologists for histopathological staging according to the UICC TNM-system[20], rescored according to the Gleason scoring system[21] and subsequently followed-up between 21 and 128 months (median 40.24 months). Three different tissue cores representing the lowest and highest Gleason grades within a single tumour were arrayed from formalin-fixed, paraffin-embedded tissue blocks using a manual device (Beecher Instruments). Two-micrometre paraffin sections were cut from every tissue microarray and used for subsequent immunohistochemical analyses within 1 week. Statistical analysis was performed with the Mann–Whitney U-Test using the SPSS 12.0 program (SPSS Inc.) and by calculating the two-tailed Spearman rank correlation coefficient. The number of cases (*n*) analysed per Gleason score (Gs) were: Gs 3 (*n* = 5); Gs 4 (*n* = 12); Gs 5 (*n* = 14); Gs 6 (*n* = 38); Gs 7 (*n* = 24); Gs 8 (*n* = 27); Gs 9 (*n* = 20); Gs 10 (*n* = 14). Normal prostate specimens (*n* = 25).

Demethylase assay and mass spectrometry analysis. The demethylation assays were performed essentially as described[1,22]. One microgram of peptide corresponding to the H3 tail residues 1–20 carrying one, two or three methyl groups at K4 in the absence or presence of a phosphorylated Thr 6, nucleosomes purified from HeLa cells, or core histones were incubated with 0.3–5 μg of bacterially expressed and purified His-LSD1, or 5 μg baculovirus-expressed and purified GST–JARID1B or GST, as indicated. Peptides were incubated for 15 min to 5 h at 37 °C in demethylation buffer containing 50 mM Tris-HCl, pH 7.5, 50 mM KCl, 5 mM MgCl$_2$ or 50 mM HEPES-KOH, pH 8.0, 2 mM ascorbate, 100 μM Fe(NH$_4$)$_2$(SO$_4$)$_2$, 1 mM α-ketoglutarate[1,22]. To phosphorylate H3T6, nucleosomes or core histones were incubated for 45 min with purified, recombinant PKCβI at 30 °C in kinase buffer. The crude demethylase reactions were diluted 1:10 in a saturated α-cyano-4-hydroxycinnamic acid solution (50% acetonitril, 0.1% trifluoroacetic acid) and spotted onto a matrix-assisted laser desorption ionisation (MALDI) target plate. For each reaction, 2,000 spectra were recorded and analysed using the Data Explorer Software.

Growth of xenograft tumours in nude and SCID mice. Five-week-old male severe combined immunodeficient (SCID) or nude mice were purchased from Charles River Laboratories. pLenti6-miRNA-control and pLenti6-miRNA-PKCβI were used to produce recombinant lentiviruses to infect LNCaP or C4-2B cells as described[17]. For tumour inoculation, 2×10^7 LNCaP or 4×10^6 C4-2B cells were injected in nude or SCID mice, respectively. Cells were resuspended in 100 μl PBS, mixed with 100 μl matrigel (BD Biosciences) on ice and administered subcutaneously in the flank of each animal. The tumour size was determined by calliper measurements twice a week[23]. All experiments were performed according to the German Animal Protection Law with permission from the responsible local authorities.

17. Wiznerowicz, M. & Trono, D. Conditional suppression of cellular genes: lentivirus vector-mediated drug-inducible RNA interference. *J. Virol.* **77**, 8957–8961 (2003).
18. O'Neill, T. E., Roberge, M. & Bradbury, E. M. Nucleosome arrays inhibit both initiation and elongation of transcripts by bacteriophage T7 RNA polymerase. *J. Mol. Biol.* **223**, 67–78 (1992).
19. Kahl, P. *et al.* Androgen receptor coactivators lysine-specific histone demethylase 1 and four and a half LIM domain protein 2 predict risk of prostate cancer recurrence. *Cancer Res.* **66**, 11341–11347 (2006).
20. Schröder, F. H. *et al.* The TNM classification of prostate cancer. *Prostate*, Suppl. 21, 129–138 (1992).
21. Hsing, A. W., Tsao, L. & Devesa, S. S. International trends and patterns of prostate cancer incidence and mortality. *Int. J. Cancer* **85**, 60–67 (2000).
22. Tsukada, Y. *et al.* Histone demethylation by a family of JmjC domain-containing proteins. *Nature* **439**, 811–816 (2005).
23. Jensen, M. M., Jørgensen, J. T., Binderup, T. & Kjaer, A. Tumor volume in subcutaneous mouse xenografts measured by microCT is more accurate and reproducible than determined by 18F-FDG-microPET or external caliper. *BMC Med. Imaging* **8**, 16 (2008).